Gradient-mixing LEGO robots for purifying DNA origami nanostructures of multiple components by rate-zonal centrifugation

Jason Sentosa[a,b,1], **Brian Horne**[c,1], **Franky Djutanta**[a,d,1,2], **Dominic Showkeir**[c,1], **Robert Rezvani**[a,c], **and Rizal F. Hariadi**[a,d,1]

[a]Biodesign Center for Molecular Design and Biomimetics (at the Biodesign Institute) at Arizona State University, Tempe, AZ 85287, USA.; [b]Department of Biomedical Engineering, Georgia Institute of Technology, GA; [c]Department of Physics, Arizona State University, AZ.; [d]School for Engineering of Matter, Transport and Energy, Arizona State University, AZ.

[1]These authors contributed equally.
[2]To whom correspondence should be addressed. E-mail: fdjutant@asu.edu AND rhariadi@asu.edu

This manuscript was compiled on July 13, 2021

Abstract

DNA origami purification is critical in emerging applications of functionalized DNA nanostructures from basic fundamental biophysics, nanorobots to therapeutics. Advances in DNA origami purification have led to the establishment of rate-zonal centrifugation (RZC) as a scalable, high-yield, and contamination-free approach to purifying DNA origami nanostructures. In RZC purification, a linear density gradient is created using viscous agents, such as glycerol and sucrose, to separate molecules based on their mass and shape during high-rpm centrifugation. However, current methods for creating density gradients are typically time-consuming because of their reliance on slow passive diffusion. Here, we built a LEGO gradient mixer to rapidly create a quasi-continuous density gradient with minimal layering of concentrations using simple rotational motion. We found that rotating two layers of different concentrations at an angle can reduce the diffusion time from a few hours to mere minutes. The instrument needed to perform the movement can be constructed from low-cost components, such as Arduino and LEGO Mindstorms pieces, and has comparable efficacy to commercial gradient mixers currently available. Our results demonstrate that the creation of a linear density gradient can be achieved with minimal labor, time, and cost with this machine. With the recent advances in DNA origami production, we anticipate our findings to further improve the viability of scaling up DNA origami purification in grams quantities. Our simple process enables automated large-scale purification of functionalized DNA origami more feasible in resource-constrained settings.

Keywords:

Frugal science, DNA nanotechnology, purification of biomolecules

Introduction

DNA origami, a facile method to self-assemble complex nanostructures from long, single-stranded DNA (scaffold strands) and programmed shorter oligonucleotides (staple strands),[1–8] has proven to be a reliable and efficient method to create nanostructures with well-defined shape and customizable geometry. The ability to fabricate the desired shapes and features of a nanoscale object offers a powerful tool for nanotechnology.[8–11] The highly specific structure of DNA origami has led to its use in fields such as medicine,[12–16] microscopy,[17–20] and electronics.[21–23] Although efforts have been made to optimize DNA

origami assembly,[24,25] the yield of well-folded origami is far less than 100%.[26] Most applications of DNA origami require uncontaminated structures that are free of staple strands and misfolded origami.[26–28] Hence, a purification step is added to isolate the well-folded structures.

Rate-Zonal Centrifugation (RZC) is a high-yield, contamination-free method of purifying DNA origami.[27] The technique employs a linear density gradient that is subjected to high centrifugal force to separate heterogeneous molecules based on their distinct mass and shape.[29] In the context of DNA origami, RZC can be used to separate well-folded structures from other undesired species (misfolded structures, staple strands, and aggregates). RZC has several advantages compared to other purification methods, such as agarose gel electrophoresis (AGE). RZC keeps the samples in aqueous solution throughout the process, is free from contaminants such as agarose gel residues, and is scalable to accommodate a large amount of sample.[27]

Although RZC may take only 1 to 3 hours and minimal labor to perform, preparing the density gradient can be time-consuming.[27,30] There are several ways to prepare a glycerol density gradient: layering two solutions of different glycerol concentrations in a tube and resting the tube horizontally for 1 to 2 hours to let the glycerol to passively diffuse, overlaying or underlaying several layers of different glycerol concentration and relying on passive diffusion, or mixing the glycerol gradient using a gradient mixer instrument. The first two methods are mostly cost-free, but time-consuming to prepare. Meanwhile, the third option is fast but requires practice and can be costly. Therefore, there is a compelling need to establish a density gradient creation method that is both fast and cost-effective to create.

Here, we report a fast and low-cost method to create a linear glycerol density gradient relying on simple rotational motion to accelerate diffusion. The instrument was made using low-cost materials from LEGO (EV3 Mindstorms). The diffusion process facilitated by the LEGO gradient mixer takes one minute, down from the several-hour process of manual methods. The general process is as follows: A low-concentration solution of glycerol is gently layered on top of a high-concentration glycerol solution inside a centrifuge tube. The glycerol-filled tubes are then loaded into the LEGO gradient mixer and the program is initiated to tilt the glycerol-filled tubes horizontally and rotate them for 1 minute at low rpm (20 rpm). The LEGO gradient mixer will return to its upright position and DNA origami samples (6-hb monomer and dimer) are loaded on top of the newly-created glycerol gradients. The tubes are then transferred to an ultracentrifuge for RZC separation.[27] Fractions are collected from the RZC result to be analyzed using AGE and the purified structures are verified using atomic force microscopy (AFM).

Materials and Methods

Buffers, reagents, materials and equipments. All buffers, reagents, materials, and equipment can be found in Section S4 of the Supporting Information.

Design of the Gradient Mixer. All components for building the LEGO gradient mixer are part of the EV3 LEGO Mindstorms kit (Item no. 31313) except the ultracentrifuge tube holder (Fig. 1a), which was 3D printed using an Ultimaker 3 3D printer (part no. 9671) (see Supplementary Fig. S1 for building instruction). The design features two motors: A spinning motor (Fig. 1b) and turning servo motor (Fig. 1c). The centrifuge tube holder is connected to the spinning motor, which is connected to the servo motor by the large grey gear (Fig. 1d). Both motors are supported by the scaffold (Fig. 1e), which connects directly to the large grey gear, allowing the spinning motor and the centrifuge tube holder to rotate into a horizontal position. Both motors are connected to the LEGO Brick (Fig. 1f), which was programmed with the protocol. When the LEGO gradient mixer is ready to be used, the servo motor slowly tilts the tubes into a horizontal position. The tubes are tilted horizontally to create greater surface area between the glycerol solutions, which accelerates diffusion. After reaching a horizontal configuration, the spinning motor begins to rotate the tubes. This allows layers of different concentrations to diffuse quickly with a smooth transition. Once the spinning motor stops, the servo motor returns the tubes back to their initial position and the gradient is ready for RZC.

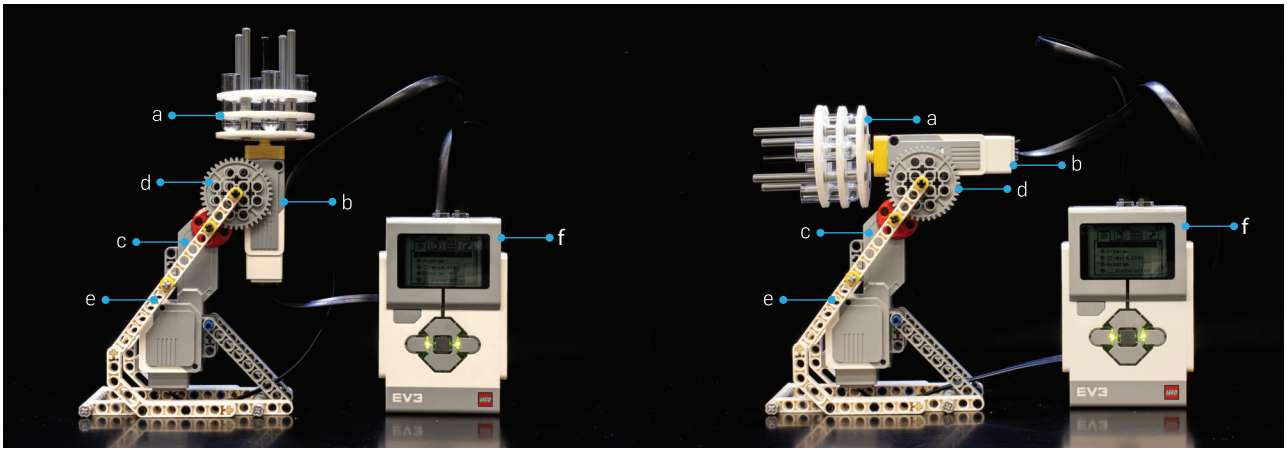

Fig. 1 Side view of the LEGO gradient mixer during its initial position (**left**) and its horizontal tilting phase (**right**). (**a**) 3D printed centrifuge-tube holder. (**b**) Spinning motor to rotate the tubes in its horizontal position. (**c**) Turning servo motor responsible for tilting the tubes horizontally. (**d**) Large grey gear connecting the two motors with its small gear complement. (**e**) The scaffold holding the structure together. (**f**) The LEGO controller for orchestrating the motions of the two motors.

DNA Origami Design and Assembly. The design for monomers and dimers was adopted from Shawn Douglas's paper,[31] which utilized a similar structure. The monomer was constructed as a single DNA origami while the dimer was constructed from two separate pieces of precursor monomer (left and right). The left and right precursor monomers were annealed individually with different staple strands such that one side of each precursor monomer was on and the other side was off. The resulting left and right monomers were filtered using a 100 kD amicon filter (4,500 ×g for 5 mins twice) to get rid of excess staples that may have prevented dimerization. The filtered products were then combined into a single tube to dimerize overnight. The CADnano file for both 6-hb monomers and dimers can be found in the Supplementary Materials Repository.

The assembly of the DNA nanostructures was accomplished in a one-pot reaction by mixing 30 nm p8094 scaffold strands and 300–900 nm staple oligonucleotides (Table S1) in a buffer solution containing 1× TAE 12.5 mM $MgCl_2$. The mixture was then annealed using a thermocycler that gradually cooled the mixture from 90 °C to 30 °C over 1.5 hours. The predicted length of a 6-hb monomer is 460 nm for 32 segments of 42 bp each, assuming the length of each base pair is 0.34 nm. The dimers have a predicted length of 920 nm with 32 segments from both the left and right part and 2/3 segment for the connectivity (total 64 2/3 segments) of 42 bp each segment. The diameter of the 6-hb origami calculated by assuming an interhelical distance of 3 nm[32] is approximately 8 nm.

Preparation of the Glycerol Gradient. A 15–45% (concentrations depend on the origami of interest) quasi-continuous glycerol gradient was prepared in the following way. First, 300 µL of 45% glycerol (v/v) in 1× TAE 12.5 mM $MgCl_2$ buffer was pipetted into a centrifuge tube. The same volume of 15% glycerol solution was then carefully layered on top of the 45% glycerol using either a dropper or a syringe to prevent disturbing the surface of the 45% glycerol (Fig. 2A.1). A clear division between the two solutions was visible. The glycerol filled centrifuge tubes were then inserted into the LEGO gradient mixer and the protocol was run to mix the layered glycerol for 1 minute, which was sufficient for the 1.0 mL tubes (Fig. 2A.2–2A.4).

The ideal spin time was discovered using a visual test. First, the 45% glycerol solution was dyed with blue food coloring. Both the clear 15% glycerol and the colored 45% glycerol (300 µL each) were added to the centrifuge tubes (Fig. 2B). The tubes were loaded into the mixer and different spin times were tested until a smooth transition from clear (15%) to blue (45%) was visible (Fig. 2C). Three other glycerol gradient concentrations (30%/45%, 15%/60%, 30%/60%) were also tested with varying spin times of 30 sec,

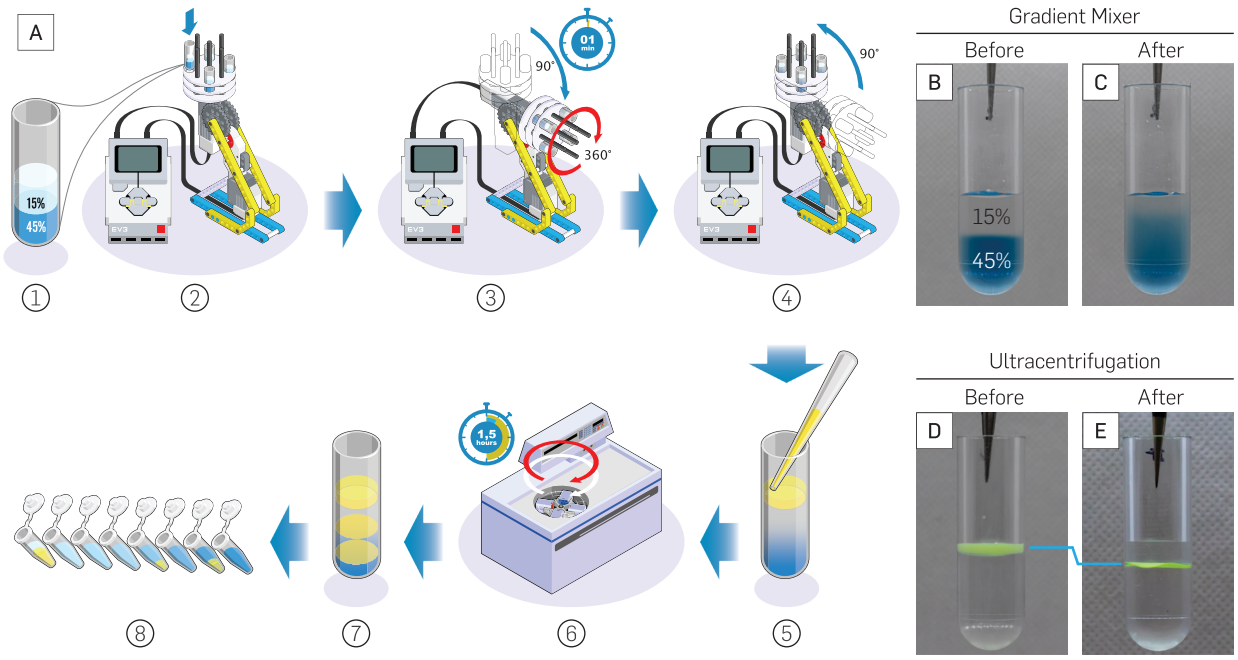

Fig. 2 **Glycerol gradient preparation and RZC purification (Movie S1).** (**A**) Preparation of glycerol gradient with LEGO gradient mixer and separation of sample by RZC. (**B**) Layers of glycerol before mixing; the blue glycerol at the bottom is 45% (v/v) and the clear glycerol at the top is 15% (v/v). (**C**) Linear glycerol gradient after mixing with LEGO gradient mixer. (**D**) 140 nm green fluorescent beads on top of the glycerol gradient before RZC. (**E**) Fluorescent beads after RZC concentrated into a thin layer due to separation from the glycerol gradient. All glycerol solutions were diluted in 1× TAE 12.5 mM $MgCl_2$

.

60 sec, 120 sec, and 180 sec. The results showed that one minute of spin time was sufficient to create the desired glycerol gradient. The 30 seconds of spin time produced a step gradient, while 120 seconds and 180 seconds of spin time produced a uniform solution rather than a gradient (Fig. 3). The detailed protocol programmed into the LEGO gradient mixer for both the experiment and the visual test can be found in the Supplementary Materials Repository.

Centrifugation and Sample Extraction Procedure. After the glycerol gradient was formed, 50-100 µL of the sample containing 10% glycerol was loaded on top of the gradient by hovering the pipette tip near the surface of the gradient (Fig. 2A.5). Most of the sample should rest on the surface of the gradient. The centrifuge tubes containing the sample and gradient were loaded into a swinging bucket rotor (Beckman TLS 55). The samples were centrifuged at 50,000 rpm (∼150,000 g) for 1.5 hours at 4° C (Fig. 2A.6). For different origami, the exact RPM and duration of centrifugation need to be optimized. Once the centrifugation was complete, 16 to 18 equal-volume fractions of the sample (Fig. 2A.7–8) were then collected from bottom to top using longneck gel-loading tips to preserve the glycerol layers (see Supplementary Movie S1 for full instructional video from gradient preparation to fractionation). Fluorescent beads (G140) were used as a control sample for RZC protocol. The beads were laid on top of the 15–45% glycerol gradient (Fig. 2D) to be centrifuged with the above protocol. The resulting tube showed the beads concentrating into a thin layer that lies below the surface where it initially was (Fig. 2E).

Experiment Calibration. Optimization of gradient parameters and centrifugation setup were done using SYBR Gold-stained sample for quick separation assessment. The sample being purified was stained with 3× SYBR Gold prior to loading into the experimented gradients. The centrifuge tubes containing the stained sample and gradient were centrifuged with the experimented setup. After centrifugation, the resulting

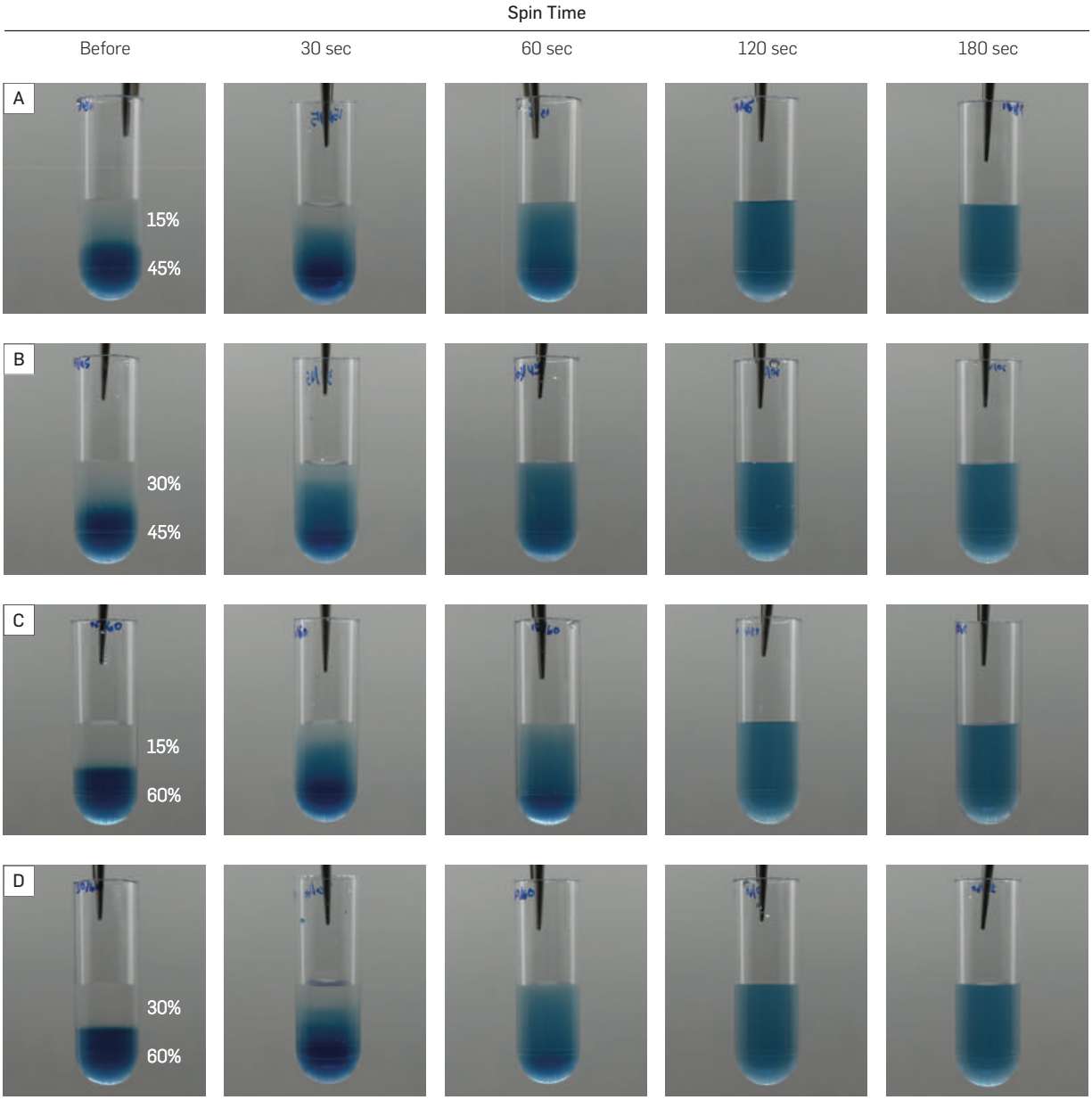

Fig. 3 **Comparison of different spin times for different gradients**. (**A**–**D**) Four different top and bottom glycerol concentration after 0, 30, 60, 120, and 180 sec. The bottom glycerol is dyed blue for visual inspection, while the top glycerol layer was kept uncolored.

tubes were visualized with Invitrogen Safe Imager 2.0 Blue Light transilluminators and the images were taken with a Canon lens EF-S 35mm f/2.8 Macro IS STM covered with a single B+W 49mm XS-Pro clear MRC-nano 007 filter on a Canon EOS 77D camera body. The structures being separated showed a thin horizontal band on the gradient while the staple strands showed a cloudy region near the top of the gradient. The best parameters were then determined by looking at the farthest separation distance between the structures being purified and the undesired molecules.

Result Confirmation and Analysis. After the centrifuged sample gradient had been partitioned into fractions, 10 μL from each fraction was taken and mixed with 1 μL of 20× SYBR gold and 1 μL of loading dye. The fractionated sample was analyzed using AGE. 6-hb monomers underwent gel electrophoresis in 1% Agarose

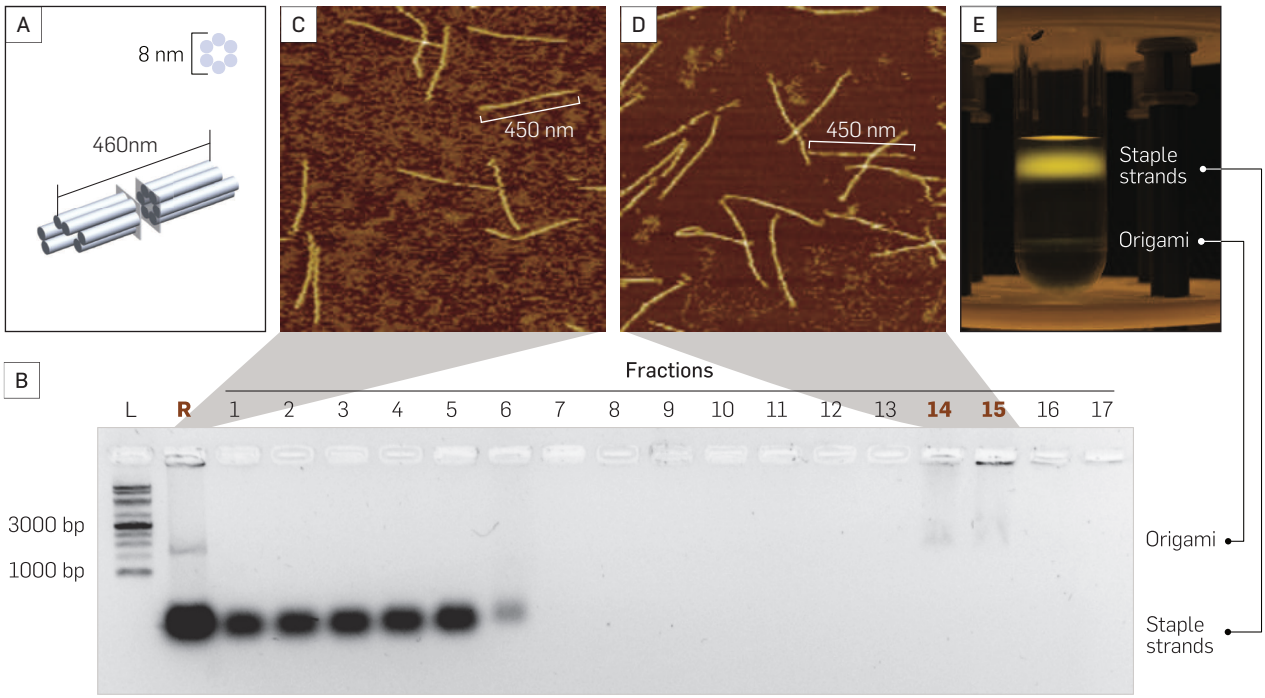

Fig. 4 **RZC purification result for 6-hb monomer**. (**A**) 3D rendered model of 6-hb monomer (not to scale; created using Solidworks). (**B**) Gel result of monomer fractions from top (1) to bottom (17). *L* is 1 kb ladder (Goldbio 1kb ladder), *R* is raw unpurified monomer, underlined fraction numbers indicate the fractions containing the purified monomer. (**C**) AFM image of the unpurified monomer. (**D**) AFM image of the RZC purified monomer. (**E**) SYBR gold stained monomer after being separated with RZC.

Gel at 75V for 1.5 hours. Once the electrophoresis was complete, the gel was post-stained with 1× SYBR gold and imaged using ultraviolet light in Bio-Rad Molecular Imager Gel Doc XR+ (1708195EDU). The AGE was done to detect the fractions containing the desired origami, which were then combined into a single tube. Buffer exchange on the purified origami is recommended to ensure the structures stay in their native buffer without any of the glycerol.

The result of the gradient purification was further confirmed by AFM imaging to compare purified and unpurified samples. Both purified and unpurified samples were diluted by 100× with 1× TAE 12.5 mM $MgCl_2$ to ensure the DNA nanotubes were sparsely distributed in the AFM scans. After preparing and calibrating the AFM, four samples were imaged: unpurified 6-hb monomer, purified 6-hb monomer, unpurified 6-hb dimer, and purified 6-hb dimer.

Statistical Analysis. The 6-hb monomer and dimer were distinguishable by their length in the AFM images, ∼500 nm for a monomer and ∼1000 nm for a dimer. The AFM images were processed in imageJ and the number of monomer and dimer were counted to calculate the content of the purified and unpurified dimers. The bootstrap method was used to calculate the standard error of mean of the content (Fig. 5I-J). The bootstrap calculation was performed with either MATLAB or Mathematica. First, the monomer and dimer were assigned as binary number 0 and 1 respectively. Then, from the full data set of sample N, a subset of size $N/2$ was randomly chosen to compute the mean. The size of the subset was rounded to the nearest integer and an element was never chosen more than once. 10,000 subsets and means were generated with randomly chosen elements each time. Finally, the standard deviation of the means were used to estimate the standard error of the monomer and dimer content.

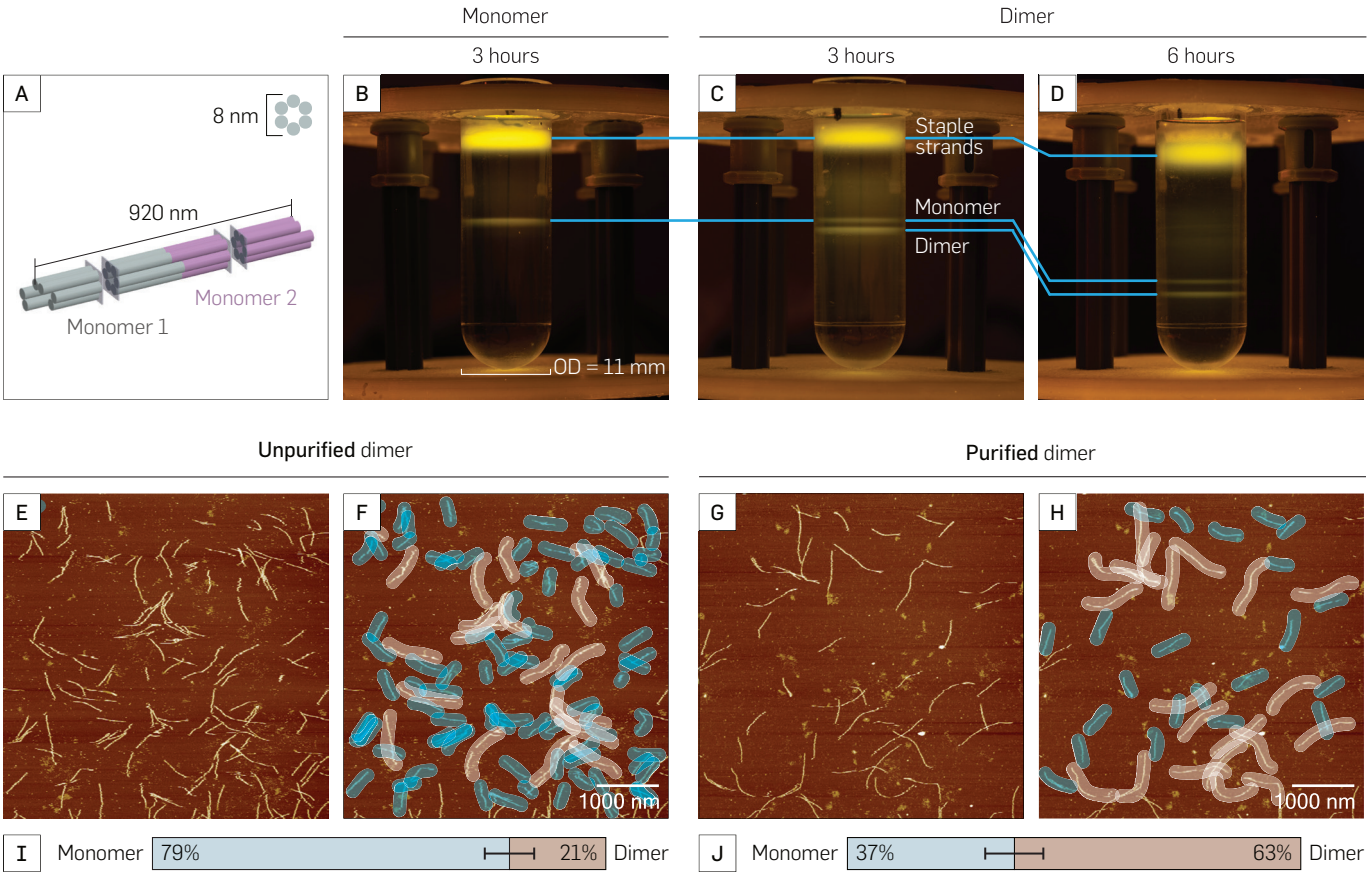

Fig. 5 **RZC purification of 6-hb dimer.** (**A**) 3D-rendered model of a 6-hb dimer (not to scale). (**B**) Comparison between SYBR gold stained 6-hb monomer (left) and (**C**) 6-hb dimer (right) purified using a 30% – 60% gradient column centrifuged for 3 hours at 50,000 rpm in 4 °C. (**D**) SYBR gold stained dimer with 6 hours of centrifugation. (**E**) AFM image of unpurified dimer. (**F**) Precursor monomer (highlighted blue) and dimer (highlighted light brown) from unpurified dimer. (**G**) AFM image of RZC purified dimer. (**H**) Significantly smaller number of monomer (highlighted blue) with similar number of dimer (highlighted light brown) compared to those in unpurified dimer. (**I** and **J**) Comparison of precursor monomers (highlighted blue) and dimer (highlighted light brown) between unpurified and purified dimer. Dimer content of unpurified dimer and purified dimer at 21±5% and 63±6% respectively. Standard deviation was calculated with the bootstrapping method (N=273 for unpurified dimer; N=114 for purified dimer).

Results

Lighter staples remain in the top section after purification. Two DNA origami structures, a 6-hb monomer (Fig. 4A) and 6-hb dimer (Fig. 5A), were purified using the glycerol gradient using the LEGO gradient mixer. The effectiveness of the gradient used for rate-zonal centrifugation was evaluated using AGE analysis and AFM imaging. The sample separation after fractionation between staples, misfolded structures, and well-folded structures was comparable to the results of other glycerol gradient preparation methods.[27] The AGE results (Fig. 4B) showed that the well-folded structures were contained in 10–20% of the glycerol gradient volume and most of the staples were accumulated near the top of the gradient, considerably separated from the origami of interest.

AFM images of the 6-hb monomer also revealed that most of the staple strands were removed after purification. The unpurified monomer AFM image surface is crowded with specs of staple strands that reside in the mixture (Fig. 4C). Conversely, the purified monomer AFM surface is much cleaner (Fig. 4D).

SYBR gold staining enables visualization of separated DNA origami. The SYBR gold-stained 6-hb monomer sample clearly showed the separation between the well-folded monomer and its excess staples using a common glycerol gradient concentration of 15% to 45% with 50,000 rpm ultracentrifuge at 4 °C for 1.5 hours (Fig. 4E).

Meanwhile, the 6-hb dimer did not show separation between the dimer and its precursor monomer with the same experimental conditions as the monomer. Fine-tuning of the experiment was done with the help of an SYBR gold visualization test. It was determined that a glycerol gradient concentration of 30% to 60% (600 μL each) spun at 50,000 rpm at 4 °C was able to separate the dimer and its precursor monomer. The dimer was compared to the monomer in the same gradient condition after 3 hours of centrifugation at 50,000 rpm at 4 °C (Fig. 5B–C). The monomer separation yielded only one thin band which corresponded to the 6-hb monomer. On the other hand, the dimer showed two bands: the upper band that was near the same level as the monomer corresponded to the precursor monomer of the dimer; the lower band corresponded to the 6-hb dimer, which has twice the mass and size of the monomer, allowing it to migrate further than the monomer during RZC. The dimer showed more separation distance from the monomer after another 3 hours of centrifugation, a total of 6 hours (Fig. 5D).

6-hb monomer structure was preserved after purification. Inspection of the DNA origami using AFM revealed that the monomer structures were not compromised (Fig. 4D) by purification. The 6-hb monomer was neither degraded nor physically altered after the purification step. This verification is important because functional DNA origami is needed for most applications. If the DNA structures are not compatible with glycerol, a buffer exchange is needed for long-term storage of the structures. Alternatively, sucrose can be used to substitute glycerol. A sucrose gradient created using the LEGO gradient mixer was able to separate the dimer with similar effectiveness to the glycerol gradient (see Figs. S2 and S3 for dimer separation using sucrose gradient).

Purification of 6-hb dimers from monomers. The AFM images reveal that separation of the dimer from its precursor monomer using the gradient from the LEGO gradient mixer was partially successful (see Supplementary Materials Repository for more AFM images of purified and unpurified 6-hb dimer). Comparison between the unpurified and purified dimer AFM images showed that there are more monomer-like structures in the unpurified dimer (79±5%; Fig. 5E–F) than in the purified dimer (37±6%; Fig. 5G–H). Percentage of DNA origami dimer over the sum of all the origami (precursor monomers and dimer) showed that the unpurified dimer (Fig. 5I) have a significantly lower dimer to monomer percentage compared to the purified dimer (Fig. 5J), 21±5% and 63±6% respectively. The non-zero monomer quantity in the dimer fraction (Fig. 5C and D) is likely due to the fluid flow during the extraction of the monomer and dimer fractions using an automatic micropipette with a long neck pipette tip.

Discussion

DNA nanotechnology has the potential to solve real-world problems in the fields of microscopy,[17–20] nanomedicine,[12–16] and even molecular-scale electronics.[21–23] Its pace toward industry applications is paired with successful efforts to remove the key obstacle of scalability for both production[33–35] and purification[27] of DNA nanostructures. The LEGO gradient mixer presented here is an effective complement to the current state-of-the-art RZC method to purify DNA origami. The LEGO gradient mixer was able to produce a concentration gradient in a relatively short timespan compared to other gradient mixers.[27,30] The gradient produced by this method was able to purify both 6-hb monomer from its staple strands and 6-hb dimer from its precursor monomer. Although the purified dimer shows only 63±6% purity (Fig. 5J), the observed monomer in the purified dimer comes from the difficulty of extracting the dimer sample manually from the small gradient volume in which the experiment is conducted. Taking note that we use less than ideal equipment for fractionation, *i.e.* long neck gel loading tips, the yield could significantly be improved by upgrading the fractionation technique. To achieve a consistent result, a better technique for fraction collection should be employed. It is also favorable to automate the fraction collection process using the

currently available liquid handling equipment for critical applications. RZC purification method paired with the gradient mixing method presented in this paper could help pave the way for large-scale DNA nanostructure production that will enable separation of functional DNA nanostructures from the side products of bioconjugation reactions, such as excess of streptavidins, quantum dots, gold nanoparticles, aptamers, and other moeties.

We note that the reported method can be further improved to reduce the cost even further. The current cost of the EV3 LEGO Mindstorms pieces used to make this device is $349.99, while the currently available gradient mixer is quoted at around $500.00 to $650.00 (Millipore Sigma gradient mixer, cat no. Z340391) and >$2K for GradientMaster (Biocomp Instruments). However, the main components of the LEGO gradient mixer are essentially a motor, a servo, and a custom holder for the tubes, all of which do not need high precision. Hence, the price to create such a machine can be reduced further by an order of magnitude (Table S2). To lower the cost further, such machine can be powered manually using some gear and scaffolding materials. In the spirit of frugal science, our discovery could help density gradient centrifugation become a more accessible tool for scientific communities around the world. The myriad applications of density gradients to fractionate DNA origami, viral particles, and a variety of macromolecules[36] have been critical in the preparation of viruses for vaccines and other immunotherapy products. The methods introduced in this paper will contribute to science education and research in resource-limited settings.

Acknowledgements

The work was initiated by a class project in PHY 472 (Advanced Biophysics Laboratory) in the Department of Physics at Arizona State University. We acknowledge other students in PHY 472, Carter Swanson, Adrian Kwiatkowski, and Biruni Hariadi for valuable discussions. We thank Sapto Cahyono for assistance with illustrations, Evangeline Taylor-Hermes for pointing the LEGO software for the building instructions, and Gde Bimananda Wisna Mahardika for technical assistance. AFM images were collected in the lab of Hao Yan at Arizona State University. The authors also thank Jeffrey La Belle's group for lending us the rotor used for ultra-centrifugation. The research in Hariadi lab was supported by the National Institutes of Health Director's New Innovator Award (1DP2AI144247), National Science Foundation SemiSynBio II (2027215), and Arizona Biomedical Research Consortium (ADHS17-00007401).

Conflict of interest

The authors have declared no competing interest.

References

1. Paul W K Rothemund. Folding DNA to create nanoscale shapes and patterns. Nature, 440(7082):297, 2006.
2. Ebbe S Andersen, Mingdong Dong, Morten M Nielsen, Kasper Jahn, Ramesh Subramani, Wael Mamdouh, Monika M Golas, Bjoern Sander, Holger Stark, Cristiano LP Oliveira, Jan Skov Pedersen, Victoria Birkedal, Flemming Besenbacher, Kurt V Gothelf, and Jørgen Kjems. Self-assembly of a nanoscale DNA box with a controllable lid. Nature, 459(7243):73–76, 2009.
3. Shawn M Douglas, Hendrik Dietz, Tim Liedl, Björn Högberg, Franziska Graf, and William M Shih. Self-assembly of DNA into nanoscale three-dimensional shapes. Nature, 459(7245):414–418, 2009.
4. Hendrik Dietz, Shawn M Douglas, and William M Shih. Folding DNA into twisted and curved nanoscale shapes. Science, 325(5941):725–730, 2009.
5. Dongran Han, Suchetan Pal, Yan Liu, and Hao Yan. Folding and cutting DNA into reconfigurable topological nanostructures. Nat Nanotechnol, 5(10):712–717, 2010.
6. Tim Liedl, Björn Högberg, Jessica Tytell, Donald E Ingber, and William M Shih. Self-assembly of three-dimensional prestressed tensegrity structures from DNA. Nat Nanotechnol, 5(7):520–524, 2010.
7. Dongran Han, Suchetan Pal, Jeanette Nangreave, Zhengtao Deng, Yan Liu, and Hao Yan. DNA origami with complex curvatures in three-dimensional space. Science, 332(6027):342–346, 2011.
8. Mark Bathe and Paul W K Rothemund. DNA nanotechnology: A foundation for programmable nanoscale materials. MRS Bull, 42(12):882–888, 2017.

9. Jeanette Nangreave, Dongran Han, Yan Liu, and Hao Yan. DNA origami: a history and current perspective. Curr Opin Chem Boil, 14(5):608–615, 2010.
10. William M Shih and Chenxiang Lin. Knitting complex weaves with DNA origami. Curr Opin Struc Biol, 20(3):276–282, 2010.
11. Thomas Tørring, Niels V Voigt, Jeanette Nangreave, Hao Yan, and Kurt V Gothelf. DNA origami: a quantum leap for self-assembly of complex structures. Chem Soc Rev, 40(12):5636–5646, 2011.
12. Rémi Veneziano, Tyson J Moyer, Matthew B Stone, Eike-Christian Wamhoff, Benjamin J Read, Sayak Mukherjee, Tyson R Shepherd, Jayajit Das, William R Schief, Darrell J Irvine, and Mark Bathe. Role of nanoscale antigen organization on b-cell activation probed using DNA origami. Nat Nanotechnol, 15(8):716–723, 2020.
13. Qian Zhang, Qiao Jiang, Na Li, Luru Dai, Qing Liu, Linlin Song, Jinye Wang, Yaqian Li, Jie Tian, Baoquan Ding, and Yang Du. DNA origami as an in vivo drug delivery vehicle for cancer therapy. ACS Nano, 8(7):6633–6643, 2014.
14. Qiao Jiang, Chen Song, Jeanette Nangreave, Xiaowei Liu, Lin Lin, Dengli Qiu, Zhen-Gang Wang, Guozhang Zou, Xingjie Liang, Hao Yan, and Baoquan Ding. DNA origami as a carrier for circumvention of drug resistance. J Am Chem Soc, 134(32):13396–13403, 2012.
15. Yong-Xing Zhao, Alan Shaw, Xianghui Zeng, Erik Benson, Andreas M Nyström, and Björn Högberg. DNA origami delivery system for cancer therapy with tunable release properties. ACS Nano, 6(10):8684–8691, 2012.
16. Joona Mikkila, Antti-Pekka Eskelinen, Elina H Niemela, Veikko Linko, Mikko J Frilander, Päivi Törmä, and Mauri A Kostiainen. Virus-encapsulated DNA origami nanostructures for cellular delivery. Nano Lett, 14(4):2196–2200, 2014.
17. Christian Steinhauer, Ralf Jungmann, Thomas L Sobey, Friedrich C Simmel, and Philip Tinnefeld. DNA origami as a nanoscopic ruler for super-resolution microscopy. Angew Chem Int Edit, 48(47):8870–8873, 2009.
18. Jürgen J Schmied, Mario Raab, Carsten Forthmann, Enrico Pibiri, Bettina Wünsch, Thorben Dammeyer, and Philip Tinnefeld. DNA origami–based standards for quantitative fluorescence microscopy. Nat Protoc, 9(6):1367–1391, 2014.
19. Sarah Helmig, Alexandru Rotaru, Dumitru Arian, Larisa Kovbasyuk, Jacob Arnbjerg, Peter R Ogilby, Jørgen Kjems, Andriy Mokhir, Flemming Besenbacher, and Kurt V Gothelf. Single molecule atomic force microscopy studies of photosensitized singlet oxygen behavior on a DNA origami template. ACS Nano, 4(12):7475–7480, 2010.
20. Ralf Jungmann, Christian Steinhauer, Max Scheible, Anton Kuzyk, Philip Tinnefeld, and Friedrich C Simmel. Single-molecule kinetics and super-resolution microscopy by fluorescence imaging of transient binding on DNA origami. Nano Lett, 10(11):4756–4761, 2010.
21. Nadrian C Seeman. DNA engineering and its application to nanotechnology. Trends Biotechnol, 17(11):437–443, 1999.
22. Albert M Hung, Christine M Micheel, Luisa D Bozano, Lucas W Osterbur, Greg M Wallraff, and Jennifer N Cha. Large-area spatially ordered arrays of gold nanoparticles directed by lithographically confined DNA origami. Nat Nanotechnol, 5(2):121–126, 2010.
23. Veikko Linko, Seppo-Tapio Paasonen, Anton Kuzyk, Päivi Törmä, and J Jussi Toppari. Characterization of the conductance mechanisms of DNA origami by ac impedance spectroscopy. Small, 5(21):2382–2386, 2009.
24. Yonggang Ke, Gaëtan Bellot, Niels V Voigt, Elena Fradkov, and William M Shih. Two design strategies for enhancement of multilayer–DNA-origami folding: underwinding for specific intercalator rescue and staple-break positioning. Chemical Sci, 3(8):2587–2597, 2012.
25. Klaus F Wagenbauer, Floris AS Engelhardt, Evi Stahl, Vera K Hechtl, Pierre Stömmer, Fabian Seebacher, Letizia Meregalli, Philip Ketterer, Thomas Gerling, and Hendrik Dietz. How we make DNA origami. ChemBioChem, 18(19):1873–1885, 2017.
26. Alan Shaw, Erik Benson, and Björn Högberg. Purification of functionalized DNA origami nanostructures. ACS Nano, 9(5):4968–4975, 2015.
27. Chenxiang Lin, Steven D Perrault, Minseok Kwak, Franziska Graf, and William M Shih. Purification of DNA-origami nanostructures by rate-zonal centrifugation. Nucleic Acids Res, 41(2):e40, 2012.
28. Christopher Timm and Christof M Niemeyer. Assembly and purification of enzyme-functionalized DNA origami structures. Angew Chem Int Edit, 54(23):6745–6750, 2015.
29. R J Britten and R B Roberts. High-resolution density gradient sedimentation analysis. Science, 131(3392):32–33, 1960.
30. Uwe Michelsen and Jörg Von Hagen. Chapter 19 isolation of subcellular organelles and structures. Method Enzymol, page 305–328, 2009.
31. Shawn M Douglas, James J Chou, and William M Shih. DNA-nanotube-induced alignment of membrane proteins

for NMR structure determination. P Natl Acad Sci USA, 104(16):6644–6648, 2007.
32. Jonathan F Berengut, Julian C Berengut, Jonathan P K Doye, Domen Prešern, Akihiro Kawamoto, Juanfang Ruan, Madeleine J Wainwright, and Lawrence K Lee. Design and synthesis of pleated DNA origami nanotubes with adjustable diameters. Nucleic Acids Res, 47(22):11963–11975, 2019.
33. Florian Praetorius, Benjamin Kick, Karl L Behler, Maximilian N Honemann, Dirk Weuster-Botz, and Hendrik Dietz. Biotechnological mass production of DNA origami. Nature, 552(7683):84–87, 2017.
34. Stefan Niekamp, Katy Blumer, Parsa M Nafisi, Kathy Tsui, John Garbutt, and Shawn M Douglas. Folding complex DNA nanostructures from limited sets of reusable sequences. Nucleic Acids Res, 44(11):e102, 2016.
35. Jean-Philippe J Sobczak, Thomas G Martin, Thomas Gerling, and Hendrik Dietz. Rapid folding of DNA into nanoscale shapes at constant temperature. Science, 338(6113):1458–1461, 2012.
36. Mohamed A Desai and Sandra P Merino. Application of density gradient ultracentrifugation using zonal rotors in the large-scale purification of biomolecules. In Downstream Processing of Proteins, pages 59–72. Springer, 2000.

Supporting Information

Gradient-mixing LEGO robots for purifying DNA origami nanostructures of multiple components by rate-zonal centrifugation

Jason Sentosa[a,b,1], **Brian Horne**[c,1], **Franky Djutanta**[a,d,1,2], **Dominic Showkeir**[c,1], **Robert Rezvani**[a,c], **and Rizal F. Hariadi**[a,d,1]

[a]Biodesign Center for Molecular Design and Biomimetics (at the Biodesign Institute) at Arizona State University, Tempe, AZ 85287, USA.; [b]Department of Biomedical Engineering, Georgia Institute of Technology, GA; [c]Department of Physics, Arizona State University, AZ.; [d]School for Engineering of Matter, Transport and Energy, Arizona State University, AZ.

[1]These authors contributed equally.
[2]To whom correspondence should be addressed. E-mail: fdjutant@asu.edu AND rhariadi@asu.edu

Contents

S1 Supplementary Figures **2**
Figure S1: LEGO building instruction . . . 2
Figure S2 . . . 2
Figure S3 . . . 2

S2 DNA sequences **4**
Table S1 . . . 4

S3 Cost analysis **6**
Table S2 . . . 6

S4 Protocols **7**
Materials . . . 7
Equipments . . . 7
Protocols . . . 8

S5 Supplementary materials repository **10**
Movie S1 . . . 10

S1. Supplementary Figures

Fig. S1 Building instruction for the LEGO gradient mixer (24 steps total) excluding the centrifuge tube holder (3D printed). Parts can be purchased from the EV3 LEGO Mindstorms kit.

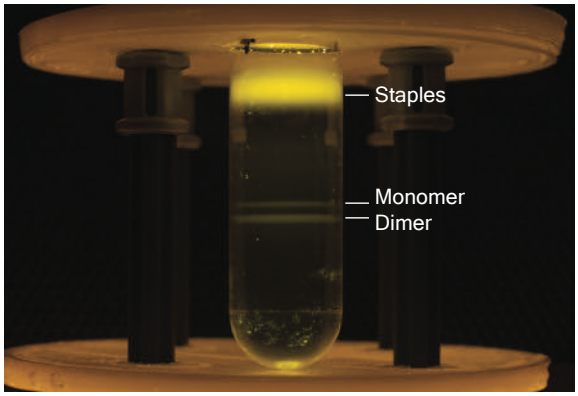

Fig. S2 Separation of dimer by RZC using 30−60% (w/v) sucrose gradient created using LEGO gradient mixer. The sample was centrifuged at 50,000 rpm at 4°C for 6 hours.

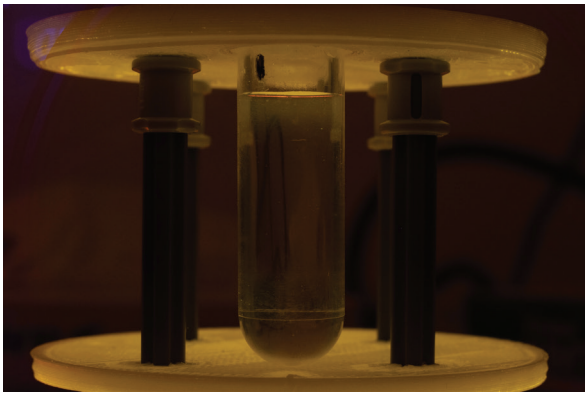

Fig. S3 RZC of SYBR gold-only sample using 30−60% (v/v) glycerol gradient. The sample was centrifuged at 50,000 rpm at 4°C for 3 hours. The SYBR gold was undetectable under blue LED illumination.

S2. DNA sequences

[h!] No	Name	Sequence
1	1[28]-5[41]-edge-ON	GGT CAG GAT TAG AGG AGC AAG AAA CAA TTT TAA GAA AAG TAA
2	2[41]-4[28]-edge-ON	AAA GCG AAC CAG ACT TCA ACA GTT TCA GGT AAA TGA ATT TTC
3	2[1343]-4[1330]-edge-ON	TGT GAG AGA TAG ACT ACG TGA ACC ATC ATA AAG CAC TAA ATC
4	1[1330]-5[1343]-edge-ON	ACC GGA AAC AAT CGT CAA TTA CCT GAG CAC CAA GTT ACA AAA
5	1[28]-5[41]-edge-OFF	TTT TTA CTC CAA CAG GTC AGG ATT AGA GGA GCA AGA AAC AAT TTT AAG AAA AGT AA
6	3[16]-2[19]-edge-OFF	TGC TAA ACA ACT CGG AAG CAA TTT TT
7	2[41]-4[28]-edge-OFF	AAA GCG AAC CAG ACT TCA ACA GTT TCA GGT AAA TGA ATT TTC TGT ATG GGA TTT TTT TT
8	5[12]-0[12]-edge-OFF	TTT TTT CTT ACC GAA GCC CTT GAA ATA GCA ATA GCT ATT TTT
9	2[1343]-4[1330]-edge-OFF	TTT TGT TTA CCA GTC CCG GAA TTT GTG AGA GAT AGA CTA CGT GAA CCA TCA TAA AGC ACT AAA TC
10	0[1355]-1[1362]-edge-OFF	TTT TTG AAT TAT TCA TTG CGA AAC GTA CAG CGC CAT TTT TT
11	1[1330]-5[1343]-edge-OFF	ACC GGA AAC AAT CGT CAA TTA CCT GAG CAC CAA GTT ACA AAA TCG CGC AGA GGC TTT TT
12	4[1360]-3[1360]-edge-OFF	TTT TTG GGG TCG AGG TGC CGC CCA AAT CAA GTT TTT TTT T
13	short 1	TAG AAT TAT TCA TTG CGA AAC GTA CAG CCC AGT CCC GGA ATT
14	short 2	TCG CGC AGA GGC TCG GGT CGA GGT GCC GCC CAA ATC AAG TTT
15	short 3	TTT GCT AAA CAA CTC GGA AGC AAG TTT AGC CAT ACT CCA ACA
16	short 4	TGT ATG GGA TTT TGT TAC CGA AGC CCT TGA AAT AGC AAT AGC
17	0[349]-2[336]	TTA GTT GCT ATT TTA AAT CAT ACA GGC ACT ATC ATA ACC CTC
18	0[685]-2[672]	CGA CAA TAA ACA ACC TGG AGC AAA CAA GAA GAA CCG GAT ATT
19	0[1021]-2[1008]	ATC GCA AGA CAA AGT GGG CGC ATC GTA AGC AAC CGC AAG AAT
20	0[391]-2[378]	AAC CTC CCG ACT TGA AAG CCT CAG AGC AAC ATA ACG CCA AAA
21	0[727]-2[714]	TAT AAA GTA CCG ACA GCA TGT CAA TCA TAG CGC AGT GTC ACT
22	0[1063]-2[1050]	GGT TGG GTT ATA TAC GAC AGT ATC GGC CCC GGA CTT GTA GAA
23	0[433]-2[420]	GAA GGC TTA TCC GGT TAT GAC CCT GTA AAT CAG TTG AGA TTT
24	0[769]-2[756]	TGT AAT TTA GGC AGC CCA AAA ACA GGA ACC TGC AGC CAG CGG
25	0[1105]-2[1092]	AAA TCA TAG GTC TGC CGG CAC CGC TTC TCT GGC AGC CTC CGG
26	0[475]-2[462]	TAG GAA TCA TTA CCA CGC AAG GAT AAA AAA ACG AAC TAA CGG
27	0[811]-2[798]	GTA GGG CTT AAT TGA ACG TTA ATA TTT TGG TGT GTT CAG CAA
28	0[1147]-2[1134]	CTT AGA TTA AGA CGC GCC ATT CAG GCT GAT TGC CGT TCC GGC
29	0[517]-2[504]	CCG CAC TCA TCG AGG CAA TGC CTG AGT ATT ATA CCA GTC AGG
30	0[853]-2[840]	GCG TTA TAC AAA TTA TCA GCT CAT TTT TTG GGT AAA GGT TTC
31	0[1189]-2[1176]	TTA ATT AAT TTT CCG GGC CTC TTC GCT ACA GGC GGC CTT TAG
32	0[559]-2[546]	TGT CTT TCC TTA TCG AAA GGC CGG AGA CAA TCA TTG TGA ATT
33	0[895]-2[882]	CCG GAA TCA TAA TTT TCG CGT CTG GCC TGT TGC GGT ATG AGC
34	0[1231]-2[1218]	ATA TAT GTG AGT GAC TGC AAG GCG ATT ATT GTG TAC ATC GAC
35	0[601]-2[588]	CAT CCT AAT TTA CGA CCG TTC TAG CTG AAC GAG TAG TAA ATT
36	0[937]-2[924]	TAC CGA CCG TGT GAA TGT GAG CGA GTA AGG GGT CAT TGC AGG
37	0[1273]-2[1260]	TCA TTT GAA TTA CCC ACG ACG TTG TAA ACA AAC TTA AAT TTC
38	0[643]-2[630]	TTA TCA ACA ATA GAT TTG AGA GAT CTA CCT CAT TCA GTG AAT
39	0[979]-2[966]	TTA GTT AAT TTC ATA CGG CGG ATT GAC CTC CCA CGC AAC CAG
40	0[1315]-2[1302]	AAA CAA ACA TCA AGT GGA GCC GCC ACG GAG GGA TAG CTC TCA
41	3[896]-1[909]	CAT AAA GTG TAA AGA TCC GCC GGG CGC GTC CTG TAG CCA GCT
42	3[1232]-1[1245]	GTT GAG TGT TGT TCC AGC AGT TGG GCG GAG TTG GGT AAC GCC
43	4[279]-0[266]	AAT AGG TGT ATC ACA GAC AAA AGG GCG AAG CCT AAT TTG CCA
44	4[615]-0[602]	GTC AGA CGA TTG GCC TCC CTC AGA GCC GGA AAA ATA ATA TCC
45	4[951]-0[938]	GTA ATA ACA TCA CTG CCG TCA ATA GAT ATT AAT GGT TTG AAA
46	4[1287]-0[1274]	AGC CGG CGA ACG TGA ACA GTA CCT TTT ATA CAT TTA ACA ATT
47	5[294]-3[307]	AGG GAG GGA AGG TAC GAG AGG GTT GAT ATC ACC CTC AGC AGC
48	5[630]-3[643]	GCC ACC CTC AGA GCC GCC AGC ATT GAC AAA GAG GAC AGA TGA
49	5[966]-3[979]	TTA GAA GTA TTA GAA ACC GTT GTA GCA AGC TTT CCA GTC GGG
50	5[1302]-3[1315]	ATA ACG GAT TCG CCA GCC CCC GAT TTA GAA AAC CGT CTA TCA
51	3[938]-1[951]	CAC ATT AAT TGC GTT GTC CAG CAT CAG CCA ACC CGT CGG ATT
52	3[1274]-1[1287]	GAA CGT GGA CTC CAC AGA AAC AGC GGA TAC GAC GGC CAG TGC
53	4[321]-0[308]	CGG ATA AGT GCC GTA ATA TTG ACG GAA ATT TTA TCC TGA ATC
54	4[657]-0[644]	ACC ACC AGA GCC GCC ACC ACC CTC AGA GCA GAA CGC GCC TGT
55	4[993]-0[980]	CCA TCA CGC AAA TTC TTT ACA AAC AAT TTT TTC AAA TAT ATT
56	4[1329]-0[1316]	GGA ACC CTA AAG GGT GAT TGC TTT GAA TAA AAG AAG ATG ATG
57	5[336]-3[349]	TGA ATT ATC ACC GTG ATT AGC GGG GTT TAC GGC TAC AGA GGC
58	5[672]-3[685]	GAT AGC CCT AAA ACA TGG CTA TTA GTC TGC TGA CCT TCA TCA
59	5[1008]-3[1021]	AAA TCC TTT GCC CGA GTG AGG CCA CCG AAT CGG CCA ACG CGC
60	0[55]-2[42]	AAG CCC AAT AAT AAA GTA CCT TTA ATT GTT AAT TCG AGC TTC
61	3[980]-1[993]	AAA CCT GTC GTG CCC GTC GGT GGT GCC AGT AAT GGG ATA GGT
62	3[1316]-1[1329]	GGG CGA TGG CCC ACT TTC TCC GTG GTG AGA ACG GAT AAC CTC
63	4[363]-0[350]	AAG AGA AGG ATT AGC ACC GAC TTG AGC CGC CTT AAA TCA AGA
64	4[699]-0[686]	GAC AAT ATT TTT GAA TCG CCA TTA AAA ATT CTG TCC AGA CGA
65	4[1035]-0[1022]	GTG TTT TTA TAA TCA ACG TTA TTA ATT TCT GAT GCA AAT CCA
66	5[42]-3[55]	GCA GAT AGC CGA ACC TTT CCA GAC GTT ACG GAG TGA GAA TAG
67	5[378]-3[391]	GCC AGC AAA ATC ACT GAA AGT ATT AAG AAA GTT TCC ATT AAA
68	5[714]-3[727]	CCA GCA GAA GAT AAA CCT GAA AGC GTA AGG CCG TTT TCA CGG
69	5[1050]-3[1063]	ACA TTA TCA TTT TGC AGG AAC GGT ACG CCA GGG TGG TTT TTC
70	0[97]-2[84]	TTG AGC GCT AAT ATG ATG GCT TAG AGC TAA AAG ATT AAG AGG
71	3[1022]-1[1035]	GGG GAG AGG CGG TTT GGT CTG GTC AGC ACC GTG CAT CTG CCA
72	4[69]-0[56]	TAA AGT TTT GTC GTA AAG TTA CCA GAA GAC AAG AAT TGA GTT
73	4[405]-0[392]	ATT ATT CTG AAA CAC AGT AGC ACC ATT AGA GGC GTT TTA GCG
74	4[741]-0[728]	ATA GAA CCC TTC TGA ACA GAG GTG AGG CCA GTA ATA AGA GAA
75	4[1077]-0[1064]	AAA GGG ATT TTA GAC GGA ACA AAG AAA CTA ACC TCC GGC TTA
76	5[84]-3[97]	GCA ATA ATA ACG GAG ACA GCC CTC ATA GAT AAT TTT TTC ACG
77	5[420]-3[433]	GGA AAC GTC ACC AAT TAA TGC CCC CTG CGG CAC CAA CCT AAA
78	5[756]-3[769]	CCG CCT GCA ACA GTA ATA AAA GGG ACA TTG CCT GTT CTT CGC
79	5[1092]-3[1105]	GAA TTA TCA TCA TAA GAG CGG GAG CTA AAT TGC CCT TCA CCG
80	0[139]-2[126]	CGG GAG AAT TAA CTA CAT GTT TTA AAT ATT ACC CTG ACT ATT
81	3[1064]-1[1077]	TTT TCA CCA GTG AGC ATA ACG GAA CGT GTC AGG AAG ATC GCA
82	4[111]-0[98]	TGT AGC ATT CCA CAA TAC CCA AAA GAA CAA GTC AGA GGG TAA
83	4[447]-0[434]	GCC CGT ATA AAC AGT GAA ACC ATC GAT AGC AAA TCA GAT ATA
84	4[783]-0[770]	GTC ACA CGA CCA GTG CCA CGC TGA GAG CTA ACA ACG CCA ACA
85	4[1119]-0[1106]	TCC TCG TTA GAA TCT TCC TGA TTA TCA GTA GTG AAT TTA TCA
86	5[126]-3[139]	CTC CTT ATT ACG CAT TTC GTC ACC AGT AAA GGA GCC TTT AAT
87	5[462]-3[475]	AGT AGC GAC AGA ATT AAC GGG GTC AGT GCA CTC ATC TTT GAC
88	5[798]-3[811]	AAA TCT AAA GCA TCT GGA TTA TTT ACA TCC CCG GGT ACC GAG
89	5[1134]-3[1147]	TCA ATA TAA TCC TGT GCT TTG ACG AGC AGT CCA CGC TGG TTT
90	0[181]-2[168]	CTT TAC AGA GAG AAT CAT TCC ATA TAA CAG TTC AGA AAA CGA
91	3[1106]-1[1119]	CCT GGC CCT GAG AGT TTT CGT CTC GTC GGG TGC CGG AAA CCA

92	4[153]-0[140]	ACC GTA ACA CTG AGG TAT GTT AGC AAA CGG AAG CGC ATT AGA
93	4[489]-0[476]	CTG GTA ATA AGT TTC AAG TTT GCC TTT ATT TTA TTT TCA TCG
94	4[825]-0[812]	TCA ATC GTC TGA AAA CCT TGC TGA ACC TGC CAA CGC TCA ACA
95	4[1161]-0[1148]	GCG CGT ACT ATG GTA TTG TTT GGA TTA TAA ACA TAG CGA TAG
96	5[168]-3[181]	CAT AAA GGT GGC AAG GAT AGC AAG CCC AGT GAA TTT CTT AAA
97	5[504]-3[517]	CGC GTT TTC ATC GGA CAT GGC TTT TGA TAA GTA CAA CGG AGA
98	5[840]-3[853]	TCA ATC AAT ATC TGG CTC ATG GAA ATA CTT TCC TGT GTG AAA
99	5[1176]-3[1189]	GAA GGG TTA GAA CCC CCG CCG CGC TTA AGG TGG TTC CGA AAT
100	0[223]-2[210]	AGA AAC GAT TTT TTG ATT TAG TTT GAC CTC GTC ATA AAT ATT
101	3[1148]-1[1161]	GCC CCA GCA GGC GAG TTA AAC GAT GCT GCG CAA CTG TTG GGA
102	4[195]-0[182]	ACC CTC ATT TTC AGC ATA TAA AAG AAA CAT GAA AAT AGC AGC
103	4[531]-0[518]	CCA GTA AGC GTC ATC ATT TTC GGT CAT ATA TTA AAC CAA GTA
104	4[867]-0[854]	GCA ACA GGA AAA ACG TCA GTT GGC AAA TGT TTA GTA TCA TAT
105	4[1203]-0[1190]	GCG TAA CCA CCA CAT ACC ATA TCA AAA TGT AAA TCG TCG CTA
106	5[210]-3[223]	GAA TAA GTT TAT TTC CTC AGA ACC GCC AAT GAC AAC AAC CAT
107	5[546]-3[559]	GTT TGC CAT CTT TTG GAA AGC GCA GTC TGA AAT CCG CGA CCT
108	5[882]-3[895]	AAT TGA GGA AGG TTA TCC AGA ACA ATA TAT ACG AGC CGG AAG
109	5[1218]-3[1231]	ACA GAA ATA AAG AAG CGC TGG CAA GTG TTA GCC CGA GAT AGG
110	0[265]-2[252]	GTT ACA AAA TAA ACA CCT GTT TAG CTA TAT AGT AAA ATG TTT
111	3[1190]-1[1203]	CGG CAA AAT CCC TTT AAA AAA AGC CGC ATT ACG CCA GCT GGC
112	4[237]-0[224]	CTC AGA ACC GCC ACT GTC ACA ATC AAT ATC CCA ATC CAA ATA
113	4[573]-0[560]	ATT AAA GCC AGA ATC ATA ATC AAA ATC AAA TCA ATA ATC GGC
114	4[909]-0[896]	GCC TTG CTG GTA ATA TCT AAA ATA TCT TAA TAA GAA TAA ACA
115	4[1245]-0[1232]	GAG CGG GCG CTA GGA TTG CGT AGA TTT TCA GTA CAT AAA TCA
116	5[252]-3[265]	TTT ACC AGC GCC AAC GTA CTC AGG AGG TGC TGA GGC TTG CAG
117	5[588]-3[601]	ACC ACC GGA ACC GCC TTG ATA TTC ACA AGC AGA CGG TCA ATC
118	5[924]-3[937]	ACT AAT AGA TTA GAT GCC TGA GTA GAA GTG AGT GAG CTA ACT
119	5[1260]-3[1273]	GAT GAA TAT ACA GTG CGA GAA AGG AAG GAG TCC ACT ATT AAA
120	0[307]-2[294]	TTA CCA ACG CTA ACG TGG CAT CAA TTC TTA GCG AGA GGC TTT
121	1[70]-5[83]	AGG TCA TTT TTG CGC AGA GAG ATA ACC CGA AAC CGA GGA AAC
122	1[406]-5[419]	TTG TAC CAA AAA CAT ATT CTA AGA ACG CCC ATT AGC AAG GCC
123	1[742]-5[755]	ATA ATC AGA AAA GCA GGC ATT TTC GAG CGG TCA GTA TTA ACA
124	1[1078]-5[1091]	CTC CAG CCA GCT TTA GAG ACT ACC TTT TCA CCA GAA GGA GCG
125	2[167]-4[154]	GAA TGA CCA TAA ATA GCT TGC TTT CGA GAT AGG AAC CCA TGT
126	2[503]-4[490]	ACG TTG GGA AGA AAC CAA GCG CGA AAC AGA TAC AGG AGT GTA
127	2[839]-4[826]	TTT GCT CGT CAT AAC ATG GTC ATA GCT GCT ACA TTT TGA CGC
128	2[1175]-4[1162]	TGA TGA AGG GTA AAA AAT CCT GTT TGA TTG CGC CGC TAC AGG
129	3[224]-1[237]	CGC CCA CGC ATA ACC CAA TAC TGC GGA AAT TAG ATA CAT TTC
130	3[560]-1[573]	GCT CCA TGT TAC TTT TAA TTT CAA CTT TAG TCA AAT CAC CAT
131	1[112]-5[125]	AAT GCT GTA GCT CAG AAC ACC CTG AAC ATG GCA TGA TTA AGA
132	1[448]-5[461]	AAG CCT TTA TTT CAG CGC CCA ATA GCA AGC AGC ACC GTA ATC
133	1[784]-5[797]	ATA TTT AAA TTG TAA GAA TCG CCA TAT TCA GCA GCA AAT GAA
134	1[1120]-5[1133]	GGC AAA GCG CCA TTC TGA GAA GAG TCA AAT GAT GGC AAT TCA
135	2[209]-4[196]	CAT TGA ATC CCC CTT AGT TGC GCC GAC ACC CTC AGA GCC ACC
136	2[545]-4[532]	ACC TTA TGC GAT TTT GAT AAA TTG TGT CCT GAA TTT ACC GTT
137	2[881]-4[868]	CGG GTC ACT GTT GCC AAT TCC ACA CAA CTA CCG CCA GCC ATT
138	2[1217]-4[1204]	ATA AAA AAA TCC CGA TAA ATC AAA AGA AAG CGG TCA CGC TGC
139	3[266]-1[279]	GGA GTT AAA GGC CGT GCC AGA GGG GGT AAT TTT CAT TTG GGG
140	3[602]-1[615]	ATA AGG GAA CCG AAC GAG AAA CAC CAG ATA AAT TAA TGC CGG
141	1[154]-5[167]	GGT GTC TGG AAG TTT AAC ATA AAA ACA GGT AGA AAA TAC ATA
142	1[490]-5[503]	CAT ATA TTT TAA ATA ACA AGC AAG CCG TGC GTC AGA CTG TAG
143	1[826]-5[839]	TAA ATT TTT GTT AAC TTA CCA GTA TAA ACA AAT ATC AAA CCC
144	1[1162]-5[1175]	AGG GCG ATC GGT GCC TTA GAA TCC TTG AAC TTC TGA ATA ATG
145	2[251]-4[238]	AGA CTG GAT AGC GTC GAT ATA TTC GGT CTT AGT ACC GCC ACC
146	2[587]-4[574]	GGG CTT GAG ATG GTA GCC GGA ACG AGG CAC AAA TAA ATC CTC
147	2[923]-4[910]	CGC TTT CGC ACT CAC CTG GGG TGC CTA AAA CTC AAA CTA TCG
148	2[1259]-4[1246]	TGC TCA TTT GCC GCC AGT TTG GAA CAA GGA AGA AAG CGA AAG
149	3[308]-1[321]	GAA AGA CAG CAT CGG ATA AAA ACC AAA AAC TAA TAG TAG TAG
150	3[644]-1[657]	ACG GTG TAC AGA CCA CGT AAC AAA GCT GAA AGG CTA TCA GGT
151	1[196]-5[209]	TCT GCG AAC GAG TAG TTT AAC GTC AAA AGC AAA GAC ACC ACG
152	1[532]-5[545]	ATT CAA AAG GGT GAA TTC CAA GAA CGG GGC CCC CTT ATT AGC
153	1[868]-5[881]	GCC ATC AAA AAT AAA CTA GAA AAA GCC TCA ACA GTT GAA AGG
154	1[1204]-5[1217]	GAA AGG GGG ATG TGA TAA CCT TGC TTC TTA TTT GCA CGT AAA
155	2[293]-4[280]	TGC AAA AGA AGT TTC TTT TGC GGG ATC GTA AGT ATA GCC CGG
156	2[629]-4[616]	AAG GCT TGC CCT GAC TGA CCA ACT TTG AGG AGG TTG AGG CAG
157	2[965]-4[952]	CTT ACG GCT GGA GGT GCG CTC ACT GCC CTA CTT CTT TGA TTA
158	2[1301]-4[1288]	CGG AAA AAG AGA CGA CGT CAA AGG GCG AAG CTT GAC GGG GAA
159	3[350]-1[363]	TTT GAG GAC TAA AGT AGT AAG AGC AAC AAG GCA AAG AAT TAG
160	3[686]-1[699]	AGA GTA ATG CTG CGT CTG TGG TCT TGA CAG AAT CGA TGA ACG
161	1[238]-5[251]	GCA AAT GGT CAA TAA GCC ATA TTA TTT AGA AAA TTC ATA TGG
162	1[574]-5[587]	CAA TAT GAT ATT CAA GCA TGT AGA AAC CCC GGA ACC AGA GCC
163	1[910]-5[923]	TTC ATC AAC ATT AAT AAA TAA GGC GTT ATA GGA GCA CTA ACA
164	1[1246]-5[1259]	AGG GTT TTC CCA GTT TTT TTA ATG GAA ACA GGT TTA ACG TCA
165	2[335]-4[322]	GTT TAC CAG ACG ACG AAC GAG GGT AGC ATG CTC AGT ACC AGG
166	2[671]-4[658]	CAT TAC CCA AAT CAA GGC GCA TAG GCT GTT AAT GCC AGA ACC
167	2[1007]-4[994]	GCC AAC GGC AGC ACA GCT GCA TTA ATG AGT AAA AGA GTC TGT
168	3[56]-1[69]	AAA GGA ACA ACT AAT CAA ATA TCG CGT TCT CCT TTT GAT AAG
169	3[392]-1[405]	CGG GTA AAA TAC GTC AAC TAA TGC AGA TTA AAG CTA AAT CGG
170	3[728]-1[741]	TCA TAC CGG GGG TTG CAT CAG ACG ATC CAT GTA CCC CGG TTG
171	1[280]-5[293]	CGC GAG CTG AAA AGG AGC GTC TTT CCA GCA TTC AAC CGA TTG
172	1[616]-5[629]	AGA GGG TAG CTA TTT AAG TCC TGA ACA ACC ACC CTC AGA ACC
173	1[952]-5[965]	CTC CGT GGG AAC AAC TTC TGA CCT AAA TAT ACA TTT GAG GAT
174	1[1288]-5[1301]	CAA GCT TTC AGA GGA AAA CAA AAT TAA TCA TCG GGA GAA ACA
175	2[377]-4[364]	GGA ATT ACG AGG CAA CTT TTT CAT GAG GGG CTG AGA CTC CTC
176	2[713]-4[700]	GCG CGC CTG TGC ACG CCA GAA TGC GGC GGA ATA CGT GGC ACA
177	2[1049]-4[1036]	CGT CAG CGT GGT GCT GCG TAT TGG GCG CCA GAA TCC TGA GAA
178	3[98]-1[111]	TTG AAA ATC TCC AAA GCG GAT TGC ATC ATA ATT GCT GAA TAT
179	3[434]-1[447]	ACG AAA GAG GCA AAA GGT AGA AAG ATT CTA CTT TTG CGG GAG
180	3[770]-1[783]	GTC CGT GAG CCT CCC AGA TGC CGG GTT AGA TTG TAT AAG CAA
181	1[322]-5[335]	CAT TAA CAT CCA ATG CAC CCA GCT ACA ATT ATT CAT TAA AGG
182	1[658]-5[671]	CAT TGC CTG AGA GTA TGT TCA GCT AAT GCC GCC ACG CGA ACT
183	1[994]-5[1007]	CAC GTT GGT GTA GAA ACG CGA GAA AAC TCG ACA ACT CGT ATT
184	2[83]-4[70]	AAG CCC GAA AGA CTA GGA ATT GCG AAT ATT AGC GTA ACG ATC
185	2[419]-4[406]	AGG AAT ACC ACA TTA ATG CCA CTA CGA ACT ATT TCG GAA CCT
186	2[755]-4[742]	TGC CGG TGC CCC CTT CTG CCA GCA CGC GTC TGG CCA ACA GAG

187	2[1091]-4[1078]	CCA GAG CAC ATC CTA CGG GCA ACA GCT GAC AGG AGG CCG ATT
188	3[140]-1[153]	TGT ATC GGT TTA TCC AAA AAT CAG GTC TTG CAA CTA AAG TAC
189	3[476]-1[489]	CCC CAG CGA TTA TAA ATC TAC GTT AAT AAT TTT TAG AAC CCT
190	3[812]-1[825]	CTC GAA TTC GTA ATA CAT CCC TTA CAC TGT TAA AAT TCG CAT
191	1[364]-5[377]	CAA AAT TAA GCA ATC GGG AGG TTT TGA AAT TTG GGA ATT AGA
192	1[700]-5[713]	GTA ATC GTA AAA CTA AAA GGT AAA GTA ATA CCG AAC GAA CCA
193	1[1036]-5[1049]	GTT TGA GGG GAC GAA CTA TAT GTA AAT GTA AAA GTT TGA GTA
194	2[125]-4[112]	ATA GTC AGA AGC AAA AAA AAG GCT CCA ACA AAC TAC AAC GCC
195	2[461]-4[448]	AAC AAC ATT ATT ACA GAA TAC ACT AAA ACC TTG AGT AAC AGT
196	2[797]-4[784]	ATC GTT AAC GGC ATT CAC AGT TGA GGA TTG GCA GAT TCA CCA
197	2[1133]-4[1120]	AAA CGC GGT CCG TTA GTT GCA GCA AGC GCG TAT AAC GTG CTT
198	3[182]-1[195]	CAG CTT GAT ACC GAC AAA TGC TTT AAA CAG TTG ATT CCC AAT
199	3[518]-1[531]	TTT GTA TCA TCG CCT AAG AAC TGG CTC AAT GTG TAG GTA AAG
200	3[854]-1[867]	TTG TTA TCC GCT CAC CTG CGG CTG GTA ATA ACC AAT AGG AAC

Table S1 Computer aided staple strand sequences for the DNA origami nanotube monomers.

S3. Cost analysis

Table S2 Estimated bill of materials for gradient mixer

Description	Purpose	Quantity	Price @	Total price
ELEGOO UNO R3 Board ATmega328P	Microcontroller	1	$ 13.99	$ 13.99
6 VDC Mini motor	Motor	1	$ 0.75	$ 0.75
SG92R Mini servo	Servo	1	$ 4.75	$ 4.75
Qunqi L298N Motor Drive Controller Board	Motor Controller	1	$ 6.69	$ 6.69
OVERTURE PLA Filament	3D Print Material	300 gr	$ 18.99 /kg	$ 6.00
			Total Price	$ 32.18

S4. Protocols

Reagents

Concentration gradient
- 50× TAE buffer, pH 8.3 (VWR Life Science, cat. no. 75800-940)
- Magnesium chloride hexahydrate (Sigma-Aldrich, cat. no. M9272)
- Glycerol (VWR Life Science, cat. no. BDH1172)
- Sucrose (Sigma-Aldrich, product no. S 0389)

DNA origami folding
- 50× TAE buffer, pH 8.3 (VWR Life Science, cat. no. 75800-940)
- Magnesium chloride hexahydrate (Sigma-Aldrich, cat. no. M9272)
- Staple strands (Integrated DNA Technique Inc.)
- ssDNA scaffold p8064 (Tilibit Nanosystem, product no. M1-51)

Agarose Gel Electrophoresis
- SYBR gold DNA gel stain (Thermo Fisher Scientific, cat no. S11494)
- DNA gel loading dye (Thermo Fisher Scientific, cat no. R0631)
- 1 kb DNA ladder (Gold Biotechnology Inc., cat. no. D010-500)
- Agarose tablets (EURx, cat. no. E0305-01)

Equipments

General
- P2L Eppendrof pipette (Gilson, SKU FA10001M)
- P10L Eppendrof pipette (Gilson, SKU FA10002M)
- P200L Eppendrof pipette (Gilson, SKU FA10005M)
- P1000L Eppendrof pipette (Gilson, SKU FA10006M)
- EXPERT tips E200 Tipack (Gilson, SKU F1733002)
- EXPERT Tips E1000 XL Tipack (Gilson, SKU F1735002)
- Milli-Q® Direct Water Purification System (Milipore Sigma, cat. no. ZR0Q016WW)

Density gradient preparation
- EV3 LEGO Mindstorm (LEGO, item no. 31313)
- Ultimaker 3 3D printer (part no. 9671)
- PLA 3D printing materials
- 1 mL syringe (Becton Dickinson, cat. no. 309628)

DNA origami preparation
- Thermocycler, MiniAmp™ Thermal Cycler REX (Thermo Fisher Scientific, cat No. A38080)
- PCR tubes (USA Scientific, cat. no. 1402-8120)
- 100 kD amicon filter (Milipore, cat. no. UFC510024)
- Benchmark MC-12 High Speed Microcentrifuge (Marshall Scientific, item no. C1612)

Rate-zonal centrifugation
- Beckman TLS 55 swinging bucket rotor (Beckman Coulter, part no. 346936)
- Polycarbonate centrifuge tube (Beckman Coulter, part no. 343778)
- Optima TLX ultracentrifuge (Beckman Coulter, part no. 361545)
- Longneck gel-loading tips (Fisher Scientific, cat. no. 02-707-81)
- Safe Imager 2.0 Blue Light transilluminators (Invitrogen, cat. no. G6600)

Gel electrophoresis
- 250 mL Erlenmeyer flask (Karter Scientific, part no. 214U2)
- External gel cast (Thermo Fisher Scientific, cat. no. B2-CST)
- Owl™ easyCast™ B2 Mini Gel Electrophoresis Systems (Thermo Fisher Scientific, cat. no. B2-BP)
- Bio-Rad Molecular Imager Gel Doc XR+ (Bio-Rad, part. no. 1708195EDU)

Atomic force microscopy
- MultiMode 8-HR AFM (Bruker)
- ScanAsyst-Fluid+probes cantilever (Bruker)
- Glass probe holder MTFML-V2 (Bruker)
- V1 AFM mica discs, 10mm (Ted Pella Inc., product no. 50-10)

- AFM/STM Metal Specimen Discs, 12mm (Ted Pella Inc., product no. 16208)

Protocols

DNA origami preparation

1 | While referring to the staple strand sequences (Table S1), pool the staple strands into the following categories.

Category	Staple Strands
Left ON	staple 1–2
Right ON	staple 3–4
Left OFF	staple 5–8
Right OFF	staple 9–12
Short 1 2	staple 13–14
Short 3 4	staple 15–16
Core 6-hb	the rest of the staples

2 | To create the 6-hb monomer mixture, combine 30 nm of the ssDNA p8064 scaffold strands and 300 nm each of the staple strands from Left OFF, Right OFF, and Core 6-hb. The strand mix should be added in 1× TAE 12.5 mM $MgCl_2$ (final concentration).

3 | To create the 6-hb dimer mixture, two types of precursor monomers mixture, *left* and *right*, need to be mixed in separate tubes. The *left* precursor monomers have complementary sequences with the *right* precursor monomer, which enable them to form a dimer. The *left* precursor monomer contains 30 nm of the ssDNA p8064 scaffold strands and 300 nm each of the staple strands in Left ON, Right OFF, Short 1 2, and Core 6-hb. The *right* precursor monomer contains 0 nm of the ssDNA p8064 scaffold strands and 300 nm each of the staple strands in Right ON, Left OFF, Short 3 4, and Core 6-hb. All origami mixture is in 1× TAE 12.5 mM $MgCl_2$ (final concentration).

4 | Anneal the 6-hb monomer, *left* precursor monomer, and *right* precursor monomer in separate PCR tubes using a thermocycler with a thermal gradient that starts at 90°C, gradually cools to 30°C over 1.5 hours, and ends with incubation at 4°C. The 6-hb monomer is formed after this annealing process. The 6-hb dimer needs an additional step after the *left* and *right* precursor monomers are formed.

5 | Filter excess staple from the *left* and *right* monomer separately using 100 kD Amicon filtration on a centrifuge. Both precursor monomers should be filtered at 4,500 g for 5 minutes twice to ensure optimal staple filtration while maintaining the DNA origami structure integrity. After filtering the mixture twice, collect the DNA origami by flipping the amicon filter on a new tube and centrifuging them at 1,000 g for 2 minutes.
CRITICAL STEP Filtration of excess staples from the precursor monomers is important to ensure the leftover staple from one precursor does not bind to the activated site of the other precursor, preventing dimerization by binding to the activated site.

6 | Combine the *left* and *right* precursor monomer after filtration of excess staples in step 5. The combined mixture is stored at 4°C to dimerize overnight. The 6-hb dimer is formed after this process.

7 | Once the 6-hb monomers and dimers are formed, perform an AGE analysis to check the formation of both origami. The monomer shows one band while the dimer shows two bands. The two bands in the dimer lane show one band at the same level as the monomer (from the precursor monomer that fails to dimerize) and another band slightly below the monomer (indicating the dimer).

Preparation of density gradient

8 | Assemble the LEGO gradient machine following the instructions in Figure S1. The LEGO parts needed to build the LEGO gradient mixer can be found in the EV3 LEGO Mindstorm pack.

9 | 3D print the centrifuge tube holder file with PLA materials. The software used to produce the .gcode needed for 3D printing is Ultimaker Cura and the 3D printer used to print the centrifuge tube holder is Ultimaker 3. Any other 3D printer can also be used to print the centrifuge tube holder. Once the centrifuge tube holder is printed, attach the

holder to the spinning motor (Figure 1b) of the LEGO assembly. The full assembly of the LEGO gradient mixer is shown in Figure 1.

10 | Prepare several different concentrations of glycerol (or sucrose, depending on the viscous agent used). A common gradient used in the experiment is a 15%–45% (v/v) gradient.

11 | Fill the centrifuge tube with 300 μL of the 45% glycerol using a pipette. Make sure that the 45% glycerol is resting on the bottom of the tube and that no bubble is present. After the 45% glycerol, lay 300 μL of 15% glycerol on top of the 45% glycerol in the centrifuge tube using a syringe to ensure minimal surface disturbance on the 45% glycerol layer. The border between the 15% and 45% glycerol should be visible.

12 | Load the glycerol-filled centrifuge tube into the designated holder in the LEGO gradient mixer. Run the LEGO_gradient_mixer_protocol.ev3 protocol found in the Supplementary Materials Repository, EV3-protocols folder. The protocol will tilt the glycerol filled tube 90°to a horizontal position and spin the tubes for one minute to mix the two different glycerol concentrations. After spinning the tubes, the LEGO gradient mixer will return the tubes to its initial position. A faded boundary and smooth gradient between the 15% and 45% glycerol can now be observed.

Rate Zonal Centrifugation and Fractionation

13 | Prepare the sample for RZC by mixing it with glycerol to a 10% (v/v) final concentration. Adding glycerol to the sample ensures the sample sits on the top surface of the glycerol gradient and eases the sample's entry into the glycerol gradient during RZC.

14 | Carefully load 50-100 μL of the sample (10% glycerol) on top of the gradient using a pipette, making sure the sample does not pierce the gradient. Most of the sample should rest on the surface of the gradient.

15 | Insert the centrifuge tubes containing the sample and gradient into a swinging-bucket rotor (Beckman TLS 55). **CRITICAL STEP** A swinging-bucket rotor should be used instead of a fixed-angle or vertical rotor because the glycerol gradient used is positioned from top to bottom. To prevent the sample from pelleting on the side and to ensure that the sample travels down the gradient, a swinging bucket rotor is needed.

16 | Centrifuge the rotor at 50,000 rpm (∼150,000 g) for 1.5 hours at 4°C in the Optima TLX ultracentrifuge. For different origami, the RPM and duration of centrifugation need to be optimized.

17 | Once the centrifugation is complete, collect 16 to 18 equal volume fractions of the gradient containing the sample. Longneck gel loading tips can be used with a pipette to fractionate the gradient from bottom to top. For a manual method such as this, fractionation from bottom to top is recommended because it ensures a more organized way to control the position of the tips. Other methods of fractionation using liquid handling instruments are preferred to achieve a more consistent RZC result.

Agarose Gel Electrophoresis

18 | After the sample has been fractionated, take 10 µL from each fraction and mix it with 1 µL of 20× SYBR gold and 1 µL of loading dye. Leave it to incubate at room temperature for 30 min.

19 | Cast a 1% agarose gel with enough lanes to accommodate the number of fractions being analyzed.

20 | When the gel is ready to use, put the gel into its electrophoresis chamber and fill the chamber with 1× TAE 12.5 mM $MgCl_2$ buffer until the gel is submerged.

21 | Load 1 kb DNA ladder and all fractions that have been labelled with SYBR gold (step 18) into their respective lanes in the gel. Start the electrophoresis using a 75 V power supply for 1.5 hours.

22 | After the gel electrophoresis is done, image the gel using Bio-Rad Molecular Imager Gel Doc XR+. Set the setting to image nucleic acids with SYBR Gold label. The bands in the gel show the staple strands near the top fraction lanes and the origami somewhere in the middle to bottom fractions. If the bands are not immediately clear,

post-staining the gel in 1× SYBR Gold for 15–30 minutes will increase the band intensity.

23 | Combine the fractions containing the origami (based on the AGE result) into a single tube which consists of the purified origami.

AFM imaging

24 | Turn on the MultiMode 8 controller and AFM to warm up the laser.

25 | Mount the 10 mm V1 mica discs onto the AFM/STM 12 mm metal specimen discs and cleave the mica sheet with a tape to an atomically-flat surface for AFM imaging.

26 | Dilute the fractionated sample by 100× with 1× TAE 12.5 mM $MgCl_2$. Depending on the purified sample concentration, the dilution factor may need to be adjusted.

27 | Pipette 30 µL of the diluted sample onto the freshly cleaved mica. More sample is sometimes added to cover the mica surface. Place the mica puck containing the sample inside the AFM.

28 | Mount the scanAsyst-Fluid+probes cantilever to the glass probe holder MTFML-V2 with a tweezer and insert them into the AFM.

29 | Lower the cantilever until it touches the sample and adjust the laser position and mirror to reach a gain of at least 6.00.

30 | Calibrate the zero position for the vertical and horizontal position and engage the cantilever to begin scanning. The scanned images are flattened and the length of the 6-hb origami(s) is measured to determine the presence of monomers (∼500 nm) and dimers (∼1000 nm).

S5. Supplementary materials repository

LEGO assembly instructions and all data supporting the findings of this study are available within the paper and in https://github.com/jsentosa/LEGO-gradient-maker.git. All raw data and AFM images are available upon request.

Movie S1 Gradient formation using the LEGO robot.
https://github.com/jsentosa/LEGO-gradient-maker/tree/master/Recording-protocols